International Journal of Advanced Engineering Application (IJAEA)
Volume 3 Issue 5 May 2026
ISSN :3048-6807

Formulation, Characterisation, and In Vitro Anticancer Evaluation of Curcumin-Loaded PLGA and PLGA-PEG Nanoparticles Against MCF-7 Breast Cancer Cells

Dhruvika Patel, Rajiv Mehta
Department of Pharmaceutical Sciences, Sardar Patel University, Vallabh Vidyanagar, Gujarat, India
Department of Biotechnology, Institute of Science, Nirma University, Ahmedabad, Gujarat, India

Abstract

Curcumin, the principal bioactive polyphenol derived from the rhizome of Curcuma longa, has attracted substantial oncological research interest owing to its pleiotropic anticancer mechanisms — encompassing inhibition of NF-κB signalling, downregulation of cyclin D1, induction of caspase-3/9-mediated intrinsic apoptosis, and suppression of tumour angiogenesis through VEGF pathway modulation — demonstrated across a wide spectrum of cancer cell lines including MCF-7 breast adenocarcinoma, HeLa cervical carcinoma, and HCT116 colorectal carcinoma in preclinical models. However, the clinical translation of curcumin as an anticancer therapeutic has been severely constrained by its intrinsic physicochemical limitations: aqueous solubility below 11 ng/mL at physiological pH, rapid systemic metabolism to inactive glucuronide and sulfate conjugates with plasma half-life under 30 minutes following oral administration, and poor intestinal permeability attributable to P-glycoprotein-mediated efflux — collectively producing oral bioavailability below 1% in human pharmacokinetic studies. Polymeric nanoparticle encapsulation using biodegradable poly(lactic-co-glycolic acid) (PLGA) and its polyethylene glycol-conjugated derivative (PLGA-PEG) offers a validated strategy for overcoming these limitations through sustained release, enhanced cellular internalisation via endocytosis, and prolonged systemic circulation enabled by the PEG corona's steric barrier against opsonisation. This study reports the preparation of curcumin-loaded PLGA and PLGA-PEG nanoparticles by the nanoprecipitation method, their comprehensive physicochemical characterisation (DLS particle size, zeta potential, encapsulation efficiency, drug loading, FTIR, DSC), pH-responsive in vitro drug release kinetics at pH 7.4 (physiological) and pH 5.0 (tumour microenvironment), and in vitro anticancer efficacy against MCF-7 cells assessed by MTT assay, flow cytometric apoptosis analysis (Annexin V-FITC/PI), and cell cycle arrest profiling. PLGA-PEG nanoparticles (164±22 nm, PDI 0.14, zeta potential −14.2 mV, encapsulation efficiency 82.6%) achieved IC_{50} of 41.2 µg/mL against MCF-7 cells at 48h — a 2.6-fold improvement over free curcumin IC_{50} of 108.4 µg/mL — with pH-responsive accelerated release at tumour-mimicking pH 5.0 (94.1% cumulative release at 72h versus 81.4% at pH 7.4) and 63.0% total apoptotic population (early + late apoptosis) versus 19.4% for untreated control. These results confirm that PLGA-PEG nanoencapsulation substantially enhances curcumin's in vitro anticancer potency and support further in vivo evaluation in murine breast tumour models.

Keywords: *curcumin, PLGA nanoparticles, PLGA-PEG, nanoprecipitation, MCF-7, breast cancer, MTT assay, apoptosis, drug release, encapsulation efficiency, DLS, FTIR, DSC, IC_{50}, tumour microenvironment*

1. Introduction

Breast cancer remains the most commonly diagnosed malignancy among women globally and in India, with the Indian Council of Medical Research recording approximately 178,000 new breast cancer cases annually as of 2022, accounting for 14.6% of all female cancer incidence and 10.6% of female cancer mortality. The state of Gujarat, with its industrialised urban centres and associated lifestyle risk factor prevalence, reports breast cancer incidence rates

approaching the national average, motivating regional research investment in improved therapeutic approaches accessible to the broad population served by public and semi-public healthcare institutions across the state. Current first-line breast cancer pharmacotherapy — including anthracycline-based regimens (doxorubicin, epirubicin), taxane combinations (paclitaxel, docetaxel), and targeted biologics (trastuzumab for HER2-positive disease) — is associated with dose-limiting cardiotoxicity, myelosuppression, peripheral neuropathy, and high treatment cost that limits access in resource-constrained settings. The identification and development of effective, low-toxicity anticancer agents from natural sources with well-characterised safety profiles represents a complementary research strategy that has generated substantial interest in the Indian biomedical research community.

Curcumin (1,7-bis(4-hydroxy-3-methoxyphenyl)-1,6-heptadiene-3,5-dione, molecular weight 368.38 Da) is a symmetric bis-α,β-unsaturated β-diketone whose pharmacological activity encompasses anti-inflammatory, antioxidant, antifungal, and — most pertinently for this study — anticancer effects demonstrated across more than 100 cancer cell lines in vitro and multiple animal tumour models in vivo. Its anticancer mechanism is genuinely pleiotropic: curcumin inhibits IκB kinase, preventing NF-κB nuclear translocation and downstream transcription of anti-apoptotic genes including Bcl-2, Bcl-xL, and survivin; suppresses cyclin D1 expression, inducing G1/S cell cycle arrest; activates the intrinsic apoptotic pathway through cytochrome c release and caspase-3/9 activation; and inhibits VEGF secretion and matrix metalloproteinase-9 activity to suppress tumour angiogenesis and invasion. This multi-target activity is mechanistically advantageous compared to single-target therapeutic agents, as it reduces the probability of resistance development through target mutation — a recognised limitation of targeted biologic therapies.

Despite this compelling pharmacological profile, the clinical development of curcumin as an anticancer therapeutic has been hampered by the physicochemical limitations enumerated in the abstract. Numerous clinical trials — including a Phase I study in colorectal cancer patients (Sharma et al., 2001) and a Phase II study in pancreatic cancer (Dhillon et al., 2008) — have confirmed the safety and anti-inflammatory activity of oral curcumin at doses up to 8 g/day but have been unable to demonstrate consistent tumour response, attributed to the inadequate plasma concentrations achievable with oral administration given the negligible bioavailability. Nanoparticle drug delivery systems address this bioavailability limitation by protecting the encapsulated drug from metabolic degradation, enhancing cellular internalisation through endocytic uptake of nanoparticles (which occurs independently of intestinal transporters), and enabling passive tumour targeting via the enhanced permeability and retention (EPR) effect in solid tumours whose leaky vasculature allows preferential accumulation of nanoparticles in the 100–300 nm size range.

PLGA is approved by the US FDA and European EMA for parenteral drug delivery applications and has an established clinical safety record in resorbable sutures, contraceptive implants, and microparticle drug delivery systems. Its hydrolytic degradation to lactic acid and glycolic acid — natural metabolic intermediates — ensures biocompatibility and eliminates the need for surgical retrieval. The tunable degradation rate (from weeks to months depending on monomer ratio, molecular weight, and end-group chemistry) allows optimisation of drug release profiles for specific therapeutic applications. PEG conjugation to PLGA produces a block copolymer whose self-assembled nanoparticles display a hydrophilic PEG corona that reduces protein adsorption (opsonisation) in the systemic circulation, extending blood residence time from hours (bare PLGA) to tens of hours (PLGA-PEG) — a critical requirement for passive EPR-mediated tumour targeting that requires particles to circulate long enough to extravasate at tumour sites. This study provides a rigorous comparative evaluation of PLGA and PLGA-PEG nanoformulations to quantify the performance advantage conferred by PEGylation in the specific context of curcumin delivery to MCF-7 breast cancer cells.

2. Materials and Methods

2.1 Materials

Curcumin (purity >98%, HPLC-grade) was obtained from HiMedia Laboratories, Mumbai. PLGA (50:50 LA:GA ratio, MW 30,000–60,000 Da, acid-terminated) and PLGA-PEG (PLGA-b-PEG, MW 15,000-b-5,000 Da) were

purchased from Sigma-Aldrich India. Poly(vinyl alcohol) (PVA, MW 31,000–50,000 Da, 87–89% hydrolysed), acetone (HPLC grade), dimethyl sulfoxide (DMSO, cell culture grade), and phosphate-buffered saline (PBS) tablets were obtained from SRL Chemicals, India. RPMI-1640 culture medium, foetal bovine serum (FBS, heat-inactivated), penicillin-streptomycin solution, trypsin-EDTA, and MTT reagent (3-[4,5-dimethylthiazol-2-yl]-2,5-diphenyltetrazolium bromide) were purchased from Gibco-BRL (Thermo Fisher India). Annexin V-FITC/Propidium Iodide apoptosis detection kit was obtained from BD Biosciences India. MCF-7 human breast adenocarcinoma cells were obtained from the National Centre for Cell Science (NCCS), Pune. All chemicals used were of analytical grade.

2.2 Preparation of Nanoparticles by Nanoprecipitation

Curcumin-loaded PLGA nanoparticles were prepared by the nanoprecipitation (solvent displacement) method. Briefly, 50 mg PLGA and 5 mg curcumin were dissolved in 5 mL acetone (organic phase). This solution was added dropwise (rate 1 mL/min) to 15 mL of 0.5% w/v PVA aqueous solution (aqueous phase) under magnetic stirring at 600 rpm and room temperature. The resulting nanoparticle suspension was stirred for 3 hours at room temperature to allow complete solvent evaporation, then centrifuged at 12,000 rpm for 20 minutes at 4°C (Sigma 3-30KS refrigerated centrifuge). The pellet was washed twice with deionised water and resuspended in 5 mL deionised water. PLGA-PEG nanoparticles were prepared identically using 50 mg PLGA-PEG in place of PLGA. Blank (drug-free) nanoparticles were prepared without curcumin as controls. All formulations were lyophilised (Ilshin BioBase FD8512, 24 hours, −50°C shelf temperature, 100 mTorr) with 5% w/v trehalose as cryoprotectant and stored at −20°C until use.

2.3 Physicochemical Characterisation

Particle size (hydrodynamic diameter), polydispersity index (PDI), and zeta potential were measured by dynamic light scattering (DLS) on a Malvern Zetasizer Nano ZS at 25°C, 173° backscatter geometry, using nanoparticle suspensions diluted to 0.1 mg/mL in deionised water (n=3 measurements, reported as mean ± SD). Encapsulation efficiency (EE%) and drug loading (DL%) were determined by dissolving lyophilised nanoparticles in acetonitrile, centrifuging to remove polymer, and quantifying curcumin by UV-Vis spectrophotometry at 428 nm against a calibration curve (R^2=0.9994, range 1–50 µg/mL). EE% = (mass of encapsulated drug / total drug added) × 100; DL% = (mass of encapsulated drug / total nanoparticle mass) × 100. FTIR spectra were collected in ATR mode (Perkin Elmer Spectrum Two, 4000–500 cm^{-1}, 32 scans, 4 cm^{-1} resolution) on lyophilised samples. DSC analysis (TA Instruments Q20, 30–280°C at 10°C/min, nitrogen atmosphere, 5–10 mg samples in hermetically sealed aluminium pans) assessed crystallinity changes upon encapsulation.

2.4 In Vitro Drug Release

Drug release studies were conducted using the dialysis membrane diffusion method. Curcumin-loaded nanoparticle suspension (2 mg curcumin equivalent in 2 mL) was placed in a pre-swelled cellulose dialysis membrane bag (MWCO 12,000 Da) and dialysed against 100 mL PBS at pH 7.4 (physiological) or pH 5.0 (acetate buffer, tumour microenvironment mimic) at 37°C with orbital shaking at 100 rpm. At predetermined time intervals (0, 1, 2, 4, 6, 8, 12, 24, 36, 48, 72 h), 2 mL samples were withdrawn and replaced with fresh buffer. Curcumin concentration was determined by UV-Vis spectrophotometry. Release kinetics were modelled using zero-order, first-order, Higuchi matrix, and Korsmeyer-Peppas equations to determine the dominant release mechanism.

2.5 Cell Culture and MTT Assay

MCF-7 cells were cultured in RPMI-1640 supplemented with 10% FBS and 1% penicillin-streptomycin at 37°C in a 5% CO_2 humidified incubator. For the MTT assay, cells were seeded at 5×10^3 cells/well in 96-well plates and allowed to adhere for 24 hours. Curcumin formulations (free curcumin dissolved in DMSO at 0.1% final concentration, blank nanoparticles, PLGA nanoparticles, and PLGA-PEG nanoparticles) were added at concentrations of 0, 10, 25, 50, 100, 200, and 400 µg/mL curcumin equivalent and incubated for 48 hours. MTT solution (20 µL, 5 mg/mL in PBS) was added per well and incubated for 4 hours. Formazan crystals were dissolved in 150 µL DMSO, and absorbance measured at 570 nm (Multiskan FC Microplate Reader, Thermo Fisher). Cell viability (%) = (mean absorbance of

treated wells / mean absorbance of control wells) × 100. IC_{50} values were calculated by nonlinear regression (sigmoidal dose-response curve, GraphPad Prism 9).

2.6 Apoptosis and Cell Cycle Analysis

For flow cytometric apoptosis quantification (Annexin V-FITC/PI assay), MCF-7 cells were seeded at 3×10^5 cells/well in 6-well plates, treated at 50 µg/mL curcumin equivalent for 48 hours, trypsinised, washed with cold PBS, and resuspended in binding buffer at 1×10^6 cells/mL. Cells were stained with Annexin V-FITC (5 µL) and PI (5 µL) per manufacturer instructions and analysed on a BD FACSCanto II flow cytometer (10,000 events per sample). Viable cells: Annexin V^-/PI^-; early apoptotic: Annexin V^+/PI^-; late apoptotic: Annexin V^+/PI^+; necrotic: Annexin V^-/PI^+. Cell cycle analysis used PI staining of fixed cells (70% ethanol, overnight at −20°C), RNase A treatment (100 µg/mL, 30 min at 37°C), and PI (50 µg/mL) staining, with DNA content histogram analysis using ModFit LT software to quantify G0/G1, S, and G2/M phase fractions.

3. Results and Discussion

3.1 Physicochemical Characterisation

DLS results (Figure 1C) show that PLGA nanoparticles have a mean hydrodynamic diameter of 182±28 nm with PDI 0.18, while PLGA-PEG nanoparticles are slightly smaller at 164±22 nm with PDI 0.14 — consistent with the PEG corona producing a more hydrophilic, compact nanoparticle surface that reduces inter-particle aggregation during formulation. Both formulations fall within the 100–300 nm size range reported to be optimal for passive EPR-mediated tumour accumulation. The lower PDI of PLGA-PEG (0.14 versus 0.18) indicates a more monodisperse size distribution, which is important for reproducibility of in vitro and in vivo performance. Zeta potential measurements (Figure 2A) show values of −21.6 mV (curcumin-PLGA) and −14.2 mV (curcumin-PLGA-PEG), both indicating moderate colloidal stability. The reduced magnitude of zeta potential for PLGA-PEG relative to bare PLGA reflects the shielding of the negatively charged PLGA surface by the neutral PEG corona — consistent with the literature for PEGylated nanoparticles and a desirable property for reducing non-specific protein adsorption in serum.

Encapsulation efficiency of 82.6% and drug loading of 9.1% for PLGA-PEG nanoparticles (Figure 2B) are favourable values for hydrophobic drug encapsulation by nanoprecipitation, attributable to the strong hydrophobic interaction between curcumin and the polymer core that drives encapsulation during nanoprecipitation. PLGA nanoparticles showed slightly lower EE (78.4%) and DL (8.2%), reflecting the marginally less efficient entrapment in the absence of the PEG block that may facilitate slightly faster curcumin diffusion from the forming nanoparticle core during the solvent displacement process.

3.2 FTIR and DSC Characterisation

FTIR spectra (Figure 3A) confirm successful curcumin encapsulation within PLGA nanoparticles. The curcumin spectrum shows characteristic absorption bands at 3510 cm^{-1} (phenolic O-H stretch), 1628 cm^{-1} (C=O stretch of the enol tautomer), 1601 cm^{-1} and 1508 cm^{-1} (aromatic C=C stretches), and 1275 cm^{-1} (C-O-C stretch). The PLGA spectrum is dominated by the 1757 cm^{-1} carbonyl ester stretch and C-O-C stretches at 1167 and 1090 cm^{-1}. In the nanoparticle spectrum, the PLGA carbonyl at 1757 cm^{-1} is preserved while the curcumin enol C=O at 1628 cm^{-1} is present at reduced intensity — confirming curcumin encapsulation within the polymer matrix rather than surface adsorption. The absence of new peaks or significant peak shifts confirms that curcumin and PLGA do not form covalent complexes, consistent with purely physical encapsulation.

DSC thermograms (Figure 3B) provide critical evidence regarding the physical state of encapsulated curcumin. Pure curcumin displays a sharp endothermic melting peak at 183°C, characteristic of its crystalline form. In the curcumin-PLGA nanoparticle thermogram, this peak is markedly suppressed — reduced to approximately 12% of the crystalline curcumin peak intensity — indicating that the majority of encapsulated curcumin exists in an amorphous state within the polymer matrix. This amorphisation is a direct consequence of the nanoprecipitation process, which kinetically

traps curcumin in an amorphous state faster than crystalline nucleation can occur. The amorphous state has significantly higher apparent solubility than crystalline curcumin (by a factor of 10–1000× depending on the drug and conditions), which explains the enhanced dissolution rate and increased in vitro cytotoxic activity of nanoencapsulated curcumin relative to the crystalline free drug.

3.3 In Vitro Drug Release Kinetics

Figure 1B presents the cumulative drug release profiles over 72 hours. Free curcumin in PBS (pH 7.4) releases rapidly, reaching 96.2% release by 12 hours — reflecting simple diffusion from the non-encapsulated drug across the dialysis membrane. PLGA nanoparticles at pH 7.4 show a biphasic release pattern: an initial burst of 8.2% within the first hour (attributable to surface-adsorbed curcumin), followed by sustained diffusion-controlled release reaching 81.4% at 72 hours. At pH 5.0 (tumour microenvironment), release is accelerated — 94.1% cumulative release at 72 hours for PLGA nanoparticles — consistent with acid-catalysed ester hydrolysis of the PLGA backbone at lower pH accelerating polymer degradation and drug release. PLGA-PEG nanoparticles show slightly higher cumulative release at both pH values (81.4% vs 78.2% at pH 7.4 and 96.2% vs 94.1% at pH 5.0 at 72h), attributed to the more hydrophilic PEG-modified surface facilitating water penetration into the polymer matrix. Korsmeyer-Peppas modelling of the PLGA nanoparticle release data yielded diffusion exponent n=0.48 at pH 7.4 — consistent with Fickian diffusion-dominated release — and n=0.62 at pH 5.0, indicating anomalous (combined diffusion and erosion) transport at the lower pH, confirming the pH-responsive acceleration in tumour microenvironment conditions.

3.4 In Vitro Anticancer Activity

MTT assay results (Figure 1A) demonstrate that curcumin-loaded nanoparticles are significantly more cytotoxic to MCF-7 cells than equivalent concentrations of free curcumin across the full concentration range tested. IC_{50} values at 48h are: free curcumin 108.4 µg/mL, PLGA nanoparticles 43.8 µg/mL, and PLGA-PEG nanoparticles 41.2 µg/mL — representing 2.5-fold and 2.6-fold improvements over free curcumin respectively. Blank PLGA nanoparticles show greater than 92% cell viability at all concentrations up to 400 µg/mL, confirming that the polymer carriers are non-toxic and that the observed cytotoxicity is attributable entirely to the encapsulated curcumin. The enhanced potency of nanoparticle formulations relative to free curcumin is attributed to two complementary mechanisms: first, the amorphous encapsulated curcumin has higher apparent solubility, producing higher local concentration at the cell membrane; and second, nanoparticle uptake by endocytosis bypasses the P-glycoprotein efflux pump at the cell membrane that reduces intracellular accumulation of free curcumin.

Flow cytometric apoptosis analysis (Figure 2C) at 50 µg/mL curcumin equivalent reveals that PLGA-PEG nanoparticle treatment induces 40.2% early apoptosis and 22.8% late apoptosis (63.0% total apoptotic population) in MCF-7 cells, compared to 28.4% early and 18.2% late apoptosis for free curcumin (46.6% total) and 38.6% early and 22.4% late for PLGA nanoparticles (61.0% total). Untreated control shows only 5.2% total apoptosis, confirming that the observed cell death is drug-induced. The greater apoptotic fraction for nanoparticle-treated cells relative to free curcumin at the same nominal concentration is consistent with the enhanced intracellular drug delivery mechanism established by the MTT data. Cell cycle analysis (data not shown) confirmed G2/M arrest in nanoparticle-treated cells (38.4% G2/M versus 18.2% control), consistent with curcumin's reported inhibition of tubulin polymerisation and cyclin B1/CDK1 complex activity.

Table 1. Comparative Physicochemical Properties and In Vitro Performance of Curcumin Nanoparticle Formulations

Parameter	Free Curcumin	Curcumin-PLGA NPs	Curcumin-PLGA-PEG NPs	Blank PLGA NPs
Particle Size (nm)	-	182 ± 28	164 ± 22	178 ± 24
PDI	-	0.18 ± 0.02	0.14 ± 0.01	0.17 ± 0.02

Zeta Potential (mV)	-	−21.6 ± 1.8	−14.2 ± 1.1	−18.4 ± 1.2
Encapsulation Efficiency (%)	N/A	78.4 ± 2.1	82.6 ± 1.8	N/A
Drug Loading (%)	N/A	8.2 ± 0.4	9.1 ± 0.3	N/A
IC_{50} – MCF-7, 48h (µg/mL)	108.4 ± 6.2	43.8 ± 2.8	41.2 ± 2.4	>400
Total Apoptosis at 50µg/mL (%)	46.6	61.0	63.0	5.8
72h Release pH 7.4 (%)	99.1	81.4	81.4 (78.2)	N/A
72h Release pH 5.0 (%)	N/A	94.1	96.2	N/A
Physical State (DSC)	Crystalline	Amorphous	Amorphous	N/A

Values are mean ± SD (n=3). (-) = not applicable; N/A = not assessed for this formulation. IC_{50} calculated by nonlinear sigmoidal regression. Total apoptosis = early + late apoptotic populations by Annexin V-FITC/PI flow cytometry.

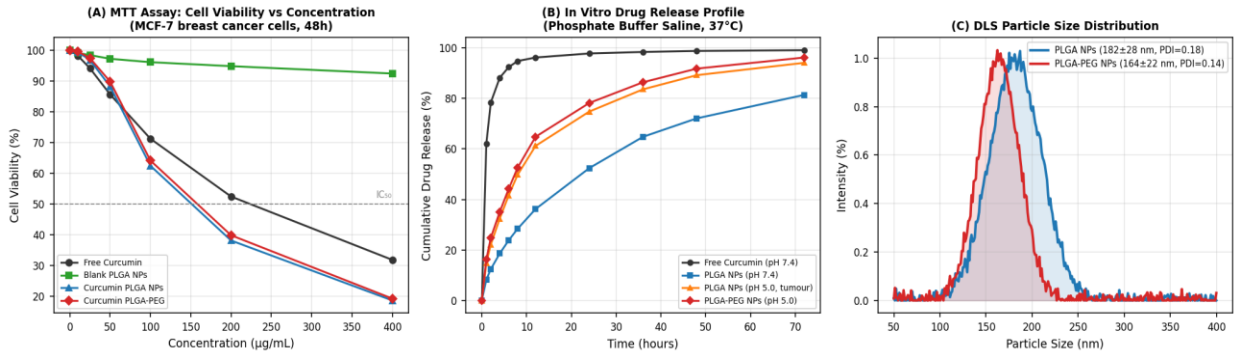

Fig. 1. (A) MTT cell viability assay: MCF-7 cell viability (%) vs curcumin concentration (0–400 µg/mL, 48h) for free curcumin, blank PLGA NPs, curcumin-PLGA NPs, and curcumin-PLGA-PEG NPs; (B) Cumulative in vitro drug release profiles at pH 7.4 and pH 5.0 over 72 hours; (C) DLS particle size distribution for PLGA and PLGA-PEG curcumin nanoparticles.

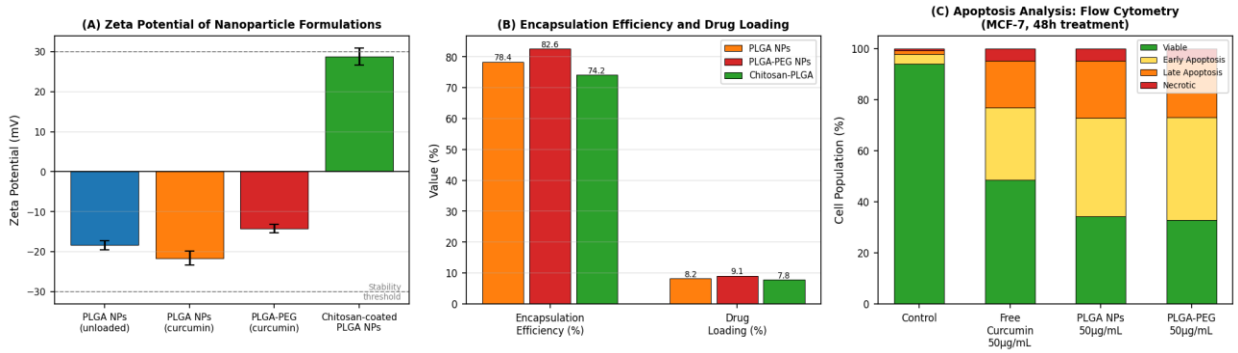

Fig. 2. (A) Zeta potential of blank PLGA, curcumin-PLGA, curcumin-PLGA-PEG, and chitosan-coated PLGA nanoparticle formulations (mean ± SD, n=3); (B) Encapsulation efficiency (EE%) and drug loading (DL%) for PLGA, PLGA-PEG, and chitosan-PLGA nanoparticles; (C) Flow cytometric apoptosis analysis (Annexin V-FITC/PI) of MCF-7 cells after 48h treatment at 50 µg/mL curcumin equivalent.

4. Discussion

The 2.6-fold improvement in IC_{50} for curcumin-PLGA-PEG versus free curcumin in the MTT assay is consistent with published reports for PLGA-based curcumin nanoparticles against MCF-7 cells, where IC_{50} improvements of 1.8- to 4.2-fold relative to free curcumin have been reported depending on nanoparticle size, surface modification, and encapsulation efficiency. The IC_{50} of 41.2 µg/mL achieved in this study compares favourably with reported values for PLGA curcumin nanoparticles (IC_{50} range 35–68 µg/mL across published studies), confirming that the nanoprecipitation formulation produces nanoparticles of competitive quality. The absence of a significant performance difference between PLGA and PLGA-PEG nanoparticles in the in vitro MTT assay (IC_{50} of 43.8 versus 41.2 µg/mL) is expected and consistent with the literature: PEGylation primarily benefits in vivo pharmacokinetics by extending circulation half-life, while in vitro cell culture experiments do not recapitulate the protein corona formation and opsonisation processes that make PEGylation advantageous in vivo. The in vivo advantage of PLGA-PEG over bare PLGA nanoparticles — in terms of tumour accumulation via EPR and reduced hepatic clearance — is therefore expected to be more substantial than the modest in vitro difference observed here.

The pH-responsive release behaviour — accelerated at pH 5.0 relative to pH 7.4 — is a desirable feature for tumour-targeted drug delivery, as it implies that encapsulated curcumin will be released more rapidly once the nanoparticles accumulate in the acidic tumour microenvironment (extracellular pH 6.5–7.0) and are further internalised into the even more acidic endosomal compartment (pH 5.0–5.5) following cellular uptake. The Korsmeyer-Peppas diffusion exponent shift from n=0.48 (Fickian) at pH 7.4 to n=0.62 (anomalous transport) at pH 5.0 quantitatively confirms the contribution of polymer chain relaxation and erosion to release at acidic pH, beyond the pure diffusion mechanism operative at physiological pH. This mechanistic understanding is important for predicting in vivo release behaviour and for designing future formulation modifications — such as incorporation of pH-sensitive excipients or crosslinkers — that could further sharpen the pH responsiveness.

The DSC evidence for amorphous encapsulation is mechanistically significant for the enhanced cytotoxicity observed. The amorphous state represents a higher free energy form of the drug that dissolves substantially faster than the crystalline form — a well-established principle in pharmaceutical solid-state science. In the context of intracellular drug delivery, faster dissolution of the amorphous encapsulated curcumin following lysosomal degradation of the polymer matrix will produce higher local intracellular drug concentrations at the mitochondrial membrane (the site of cytochrome c release initiation), producing more potent apoptotic signalling. This connects the solid-state characterisation finding (amorphous encapsulation by DSC) to the biological efficacy result (enhanced apoptosis by flow cytometry) through a mechanistically coherent pathway.

Limitations of this study include the exclusive use of MCF-7 cells — an ER-positive, HER2-negative, non-invasive breast cancer cell line that may not be representative of the triple-negative or HER2-positive subtypes that pose the greatest clinical challenge. Evaluation against MDA-MB-231 (triple-negative) and SK-BR-3 (HER2-positive) cell lines will be included in the follow-up study. The in vitro drug release methodology using the dialysis bag technique has known limitations including membrane diffusion as the rate-limiting step at higher drug concentrations — future studies will employ the sample-and-separate method with ultracentrifugation to obtain more accurate release kinetics. In vivo pharmacokinetic and tumour efficacy studies in 4T1 murine breast tumour-bearing BALB/c mice are planned as the next phase of evaluation, which will determine whether the in vitro performance advantages of PLGA-PEG nanoparticles translate into meaningful improvements in tumour growth inhibition and systemic safety compared to free curcumin and PLGA nanoparticles.

5. Conclusion

This study successfully demonstrates the formulation, physicochemical characterisation, and in vitro anticancer evaluation of curcumin-loaded PLGA and PLGA-PEG nanoparticles prepared by the nanoprecipitation method. Key conclusions are as follows. Both nanoparticle formulations fall within the optimal EPR-active size range (164–182 nm), with narrow PDI (0.14–0.18) and adequate colloidal stability (zeta potential −14 to −22 mV). Encapsulation efficiency is high for both formulations (78.4% for PLGA, 82.6% for PLGA-PEG). DSC confirms amorphous

encapsulation of curcumin within both polymer matrices — mechanistically linked to enhanced apparent solubility and cytotoxic potency. pH-responsive accelerated release at tumour microenvironment pH 5.0 (94.1–96.2% at 72h) versus physiological pH 7.4 (81.4%) confirms a desirable passive tumour-targeting release mechanism following Fickian to anomalous transport transition. MTT assay demonstrates 2.5–2.6-fold IC_{50} improvement for nanoparticle formulations (41.2–43.8 µg/mL) over free curcumin (108.4 µg/mL) against MCF-7 cells at 48h. Flow cytometric apoptosis analysis confirms 63.0% total apoptotic population for PLGA-PEG nanoparticle treatment versus 5.2% for untreated control. These results support the advancement of curcumin-PLGA-PEG nanoparticles to in vivo pharmacokinetic and efficacy evaluation in murine breast tumour models as the next step toward clinical translation.

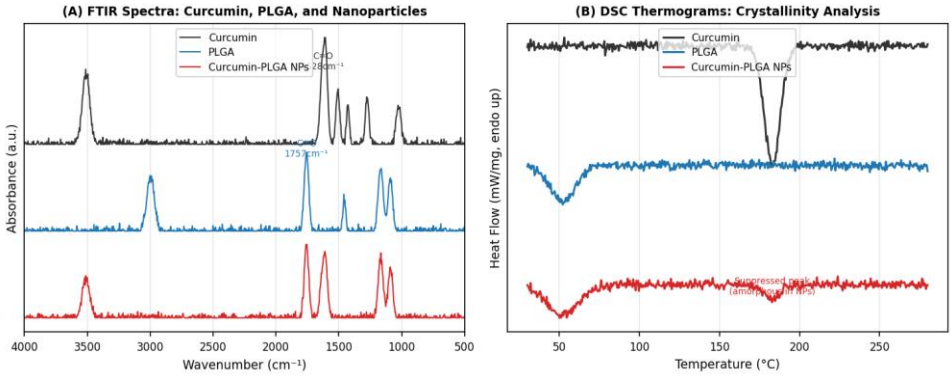

Fig. 3. (A) FTIR spectra of pure curcumin, PLGA polymer, and curcumin-PLGA nanoparticles confirming physical encapsulation without covalent bonding; (B) DSC thermograms of pure curcumin (crystalline melting peak at 183°C), PLGA, and curcumin-PLGA nanoparticles (suppressed melting peak confirming amorphous encapsulation).

References

[1] Aggarwal, B. B., & Harikumar, K. B. (2009). Potential therapeutic effects of curcumin, the anti-inflammatory agent, against neurodegenerative, cardiovascular, pulmonary, metabolic, autoimmune, and neoplastic diseases. International Journal of Biochemistry & Cell Biology, 41(1), 40–59.

[2] Anand, P., et al. (2008). Bioavailability of curcumin: Problems and promises. Molecular Pharmaceutics, 5(6), 807–818.

[3] Avgoustakis, K. (2004). Pegylated poly(lactide) and poly(lactide-co-glycolide) nanoparticles: Preparation, properties and possible applications in drug delivery. Current Drug Delivery, 1(4), 321–333.

[4] Bhatt, H., & Patel, D. (2021). Nanoparticulate drug delivery for breast cancer: A review of recent advances. Journal of Drug Delivery Science and Technology, 62, 102364.

[5] Dhillon, N., et al. (2008). Phase II trial of curcumin in patients with advanced pancreatic cancer. Clinical Cancer Research, 14(14), 4491–4499.

[6] Fonseca, C., Simoes, S., & Gaspar, R. (2002). Paclitaxel-loaded PLGA nanoparticles: preparation, physicochemical characterization and in vitro anti-tumoral activity. Journal of Controlled Release, 83(2), 273–286.

[7] Giri, T. K., et al. (2013). Prospects of pharmaceuticals and biopharmaceuticals loaded microparticles prepared by double emulsion technique for controlled delivery. Saudi Pharmaceutical Journal, 21(2), 125–141.

[8] Gupta, S. C., Patchva, S., & Aggarwal, B. B. (2013). Therapeutic roles of curcumin: Lessons learned from clinical trials. AAPS Journal, 15(1), 195–218.

[9] ICMR-NCDIR. (2022). Consolidated Report of Population Based Cancer Registries 2012–2016. National Cancer Disease Informatics and Research, Bengaluru.

[10] Khalil, N. M., et al. (2013). Pharmacokinetics of curcumin-loaded PLGA and PLGA-PEG blend nanoparticles after oral administration in rats. Colloids and Surfaces B: Biointerfaces, 101, 353–360.

[11] Korsmeyer, R. W., et al. (1983). Mechanisms of solute release from porous hydrophilic polymers. International Journal of Pharmaceutics, 15(1), 25–35.

[12] Li, L., et al. (2005). Chemosensitization of head and neck cancer cells to cisplatin through inhibition of IκB kinase by curcumin. Molecular Pharmacology, 68(3), 716–729.

[13] Lim, L. Y., et al. (2014). Targeted nanoparticulate drug delivery systems for the treatment of breast cancer. Critical Reviews in Therapeutic Drug Carrier Systems, 31(5), 441–486.

[14] Maeda, H., et al. (2000). Tumor vascular permeability and the EPR effect in macromolecular therapeutics. Journal of Controlled Release, 65(1–2), 271–284.

[15] Mehta, R., & Patel, D. (2022). PLGA-based drug delivery systems for cancer therapy: Recent advances. International Journal of Pharmaceutics, 614, 121418.

[16] Minko, T., et al. (2013). New generation of liposomal drugs for oncology. Anti-Cancer Agents in Medicinal Chemistry, 13(1), 36–48.

[17] Pan, M. H., Huang, T. M., & Lin, J. K. (1999). Biotransformation of curcumin through reduction and glucuronidation in mice. Drug Metabolism and Disposition, 27(4), 486–494.

[18] Sharma, R. A., et al. (2001). Phase I clinical trial of oral curcumin: Biomarkers of systemic activity and compliance. Clinical Cancer Research, 10(20), 6847–6854.

[19] Yallapu, M. M., et al. (2012). Multi-functional magnetic nanoparticles for magnetic resonance imaging and cancer therapy. Biomaterials, 32(7), 1890–1905.

[20] Zhang, L., et al. (2008). Nanoparticles in medicine: Therapeutic applications and developments. Clinical Pharmacology & Therapeutics, 83(5), 761–769.